A NIGHT-TIME MEASUREMENT OF OZONE ABOVE 40 KM

by

Edith I. Reed and Reuben Scolnik
Goddard Space Flight Center
National Aeronautics and Space Administration
Greenbelt, Maryland

A NIGHT-TIME MEASUREMENT OF OZONE ABOVE 40 KM

by
Edith I. Reed and Reuben Scolnik
Goddard Space Flight Center
National Aeronautics and Space Administration
Greenbelt, Maryland

ABSTRACT

The ozone distribution between 40 and 70 km was measured near midnight, May 27, 1960, from Wallops Island, Virginia by means of photometers sensitive to the ultraviolet airglow at wavelengths between 2400 and 2900 A. Below 60 km, the densities are within a factor of two of the daytime photochemical equilibrium, as represented by Johnson's late afternoon measurement of June 14, 1949. Above 60 km, the ozone density increased with altitude, with its maximum increase, a factor of 6 over the day time value, occurring at 63 km.

INTRODUCTION

At high altitudes, above the principal ozone maximum, ozone concentration as a function of altitude should be governed principally by the presence or absence of sunlight, and vary in a predictable manner from day to night and from season to season [Chapman, 1930a,b]. The first direct measurement of the daytime profile was a result of studies of the sun conducted by the Naval Research Laboratory on a V-2 rocket in 1949. Ozone densities up to 70 km were deduced from solar spectra and were consistent with computed photoequilibrium profiles [Johnson, et al, 1952]. Chapman also suggested that at high altitudes, above the ozone maximum and below the atomic oxygen maximum, ozone would increase at night as a result of a reaction between atomic and molecular oxygen. Several have treated this problem numerically, including Nicolet [1957], Barth [1961], Dütsch [1961], Paetzold [1961], Wallace [1962], and Hunt [1964], but with varying results, depending on the set of reactions, reaction rates, and initial concentrations which were chosen. Of particular difficulty is the computation of the effects of minor constituents such as hydrogen, nitrogen oxides, and the hydroxyl radical.

Ground based measurements of ozone content at these altitudes have not been satisfactory. Measurements of total ozone content are not particularly helpful since

[redacted]

variations in the ozone content below 30 km due to air movements are comparable to the expected night time increase at higher altitudes. However, the discovery of the ultraviolet airglow and a general improvement in the techniques of ultraviolet photometry made a night time measurement of ozone feasible.

In 1957, the Naval Research Laboratory flew an ultraviolet photometer with a response from 2600 to 2900 A, and did observe an ultraviolet airglow layer centered at 101 km [Tousey, 1958]. This had been predicted from laboratory observations which showed that the Herzberg bands of molecular oxygen, the visible end of which had been observed in the airglow [Chamberlain, 1955], extend to 2563 A in the ultraviolet [Broida and Gaydon, 1954]. But because an unknown amount of the observed airglow could be due to an OI line at 2972 A, where the filter transmission is still 10% of its maximum; the ozone density could not be determined unambiguously.

In May 1960, Goddard Space Flight Center flew a number of ultraviolet photometers, including some whose filters were centered at 2620 A and narrow enough so that the absorption cross section of ozone varied by only 50% over the bandwidth of the filter. These data, when interpreted with the aid of an airglow spectrum obtained by T. Stecher (of GSFC), provide an ozone density profile between 40 and 70 km.

INSTRUMENTATION

NASA Aerobee 4.05, one of a series of payloads designed for stellar photometry [Boggess, 1961], contained three pairs of photoelectric photometers, each pair mounted 120 degrees apart around the rocket axis (See Figure 1) looking out at three different angles to that axis: nominally, 75°, 90°, and 105°. One photometer of each pair was sensitive to light in the spectral region centered near 2620 A, while the response of the other was centered near 2260 A, but with their optical axes parallel. Each pair was mounted on a removable door, which, when installed, became an integral part of the rocket skin. Since the principal purpose of this instrumentation was ultraviolet star spectroscopy, 2620 A photometers were preferred to the 2680 A ones (to reduce ambiguity in the interpretation of stellar data due to the strong magnesium doublet at 2800 A). However, to correlate the data from this flight with that of earlier flights, one 2680 A photometer was included. This was mounted on the door containing the 90° photometers, and also looked at 90° with respect to the rocket axis.

The optical system of each photometer was similar and is shown in Figure 2. Calcium fluoride was used for all lenses in the 2260 A units; quartz for those in the 2620 and 2680 A photometers. The field of view had a total width of between 4 to 5°.

Isolation of the 2600 A region was achieved by combining two millimeters of 0.05% lead-doped KCl:KBr (1:1) crystal with Cation-X in thin sheets of polyvinyl alcohol [Childs, 1961]. Three millimeters of nickel sulfate hexahydrate provided a sharp cutoff for longer wavelengths; one Corning #7-54 and one Corning 9-54 filter sharpened the shorter wavelength cutoff. A typical filter had a transmittance of 0.18, an effective wavelength of 2620 A and a 200 A bandwidth.

The 2700 A filter consisted of three Corning 7-54 filters, one sheet of Cation-X and 5 millimeters of nickel sulfate hexahydrate. It had an effective wavelength of 2680 A, a transmittance of 0.16, and a bandwidth of 320 A.

The relative spectral response of the filters (see Figure 4) was measured by C. Childs, formerly of this laboratory, with a recording spectrophotometer, Cary Model #14, with an analytical accuracy of ½ of 1% for relative spectral transmission, a wavelength calibration of 4A, and a resolving power of 1A. Over the wavelength regions covered by each filter, the photomultiplier was assumed to have a constant sensitivity and the lenses a constant transmissivity. The relative response of the photometers was determined by use of the 2537 A line, to which all three types of photometers respond with an easily measured signal.

The 2530 A photometer used RCA's well-known 1P28 as a detector; all others used EMI's 6256B, an end-on fused silica window multiplier with cesium antimonide photocathode. A solenoid-operated shutter between the field stop and multiplier gave optical zero signals several times during the flight. The 1P28 and 6256B's were operated at 1000 and 1800 volts respectively; each detector had its own solid state DC to DC inverter power source with a resistor divider network at the base of each multiplier.

Each photomultiplier output was amplified to the zero to five volt range required by the telemetry system with what was essentially an impedance converter. Designed by G. Baker of this laboratory, the converter-amplifier had an electrometer tube (5886) input stage and ended with an emitter follower, with an over-all voltage gain of 2.5 for small signals. It was purposely non-linear in order to extend the dynamic range. A typical calibration curve is shown in Figure 3. The output voltage went directly to a pulse position modulation telemetry transmitter which relayed the data to the ground receiving equipment.

<u>BASIC DATA</u>

Aerobee-Hi NASA 4.06 was launched at 0250 EST on May 27, 1960 from Wallops Island, Virginia (37°50' N, 75° 29' W). The vehicle performance was normal; propulsion ended at 52.4 sec after launch at an altitude of 36.8 km

with a vertical velocity of [illegible] km/sec and a horizontal velocity of .286 km/sec at an azimuth of 311°. The rocket spun about its longitudinal axis at a rate of 1.15 rps and soon entered a precession cone of 5.7° half angle, whose axis was 16.8° from zenith at an azimuth of 25°, with a period of 75 sec. Aspect during the ascent and free-fall portions of the flight was determined from a combination of data from magnetometers, long-term integration, and horizon and star data from the photometers. Re-entry aspect could not be determined with useful accuracy [illegible] the free-fall region. A peak altitude of 175.8 ± 0.8 km was reached 249.4 seconds after launch. Telemetry ceased at 463 sec; no recovery of instrumentation was attempted.

In Figure 5 is a sample of the telemetry record from two of the photometers for [illegible] corresponding to [illegible] revolutions of the vehicle, while the airglow layer is still above the rocket. Since these photometers are nearly perpendicular to the rocket axis, the zenith angle of the photometer axis changes from a minimum (75° for the [illegible] in Figure 5) as the photometer points skywards, through 90° as it scans the horizon, and to a maximum of 105° as it points earthward. Ozone is relatively opaque around 2000 Å, and the airglow in Figure 5 can be seen only when the zenith angle of the photometer is near a minimum.

The ozone is relatively transparent to the light passed by the 2260 A filter, and the brightening of the airglow at the horizons can be clearly seen. (The light is probably of wavelengths longer than 2700 A, passed through the long wavelength tail of the 2260 A filter.) The southern horizon appears wider because it is merged with several bright stars in the Milky Way. As the vehicle increased in altitude, the signal from the 2620 A photometer resembled that from the 2260 A photometer, with bright horizons, a less bright sky toward zenith, and a dark earth. Above the airglow layer, the sky was dark (except for the brighter stars) and the earth appeared light. The noise in the record is due partly to the photomultiplier and partly to stars. The records were read at the midpoint between horizons, and analyzed to yield both a distribution of ozone with altitude and the volume emission of the airglow versus altitude.

The data obtained in the region of interest is shown in Figure 6. Data from 3 of the 7 photometers proved to be useful for ozone measurements. The pass band of the three 2260 A photometers was too wide to permit an accurate determination of an effective cross section for ozone; the down looking 2620 A photometer could not see the airglow while the vehicle was below the airglow layer. Data points for the photometers are shown to indicate the scatter in the raw data. As would be expected, the scatter increased

rapidly as the signal rose into the non-linear portion of the amplifier response curve. In addition to the data, the angle of the rocket's longitudinal axis with respect to local zenith is given. The rocket took a spiral path with an zenith angle of 8^{o} at thrust termination (52.4 sec) until it entered its regular precession cone of motion at about 75 seconds.

OZONE

The ozone content of the atmosphere is obtained from the rate of increase of the airglow signal as the vehicle rose. The energy observed is related to the ozone density in the following manner:

$$n(O_3) = \frac{(\log E_2 - \log E_1)\, n \cos \gamma}{a\,(h_2 - h_1)}$$

where $n(O_3)$ is the number of ozone molecules per cm^3

h_1 and h_2 are the lower and upper ends of the altitude interval,

E_1 and E_2 are energies observed at the corresponding altitudes,

n is Loschmidt's number, 2.687×10^{19} cm^{-3},

γ is the angle between the photometer axis and zenith, and

a is the absorption coefficient, cm^{-1}, base 10.

ozone absorption coefficient are sufficiently well known such that they contribute no more than a total of about 20% uncertainty to the number density of ozone. This would be a systematic error which would not affect the shape of the curve.

The angle of the photometers with respect to zenith could easily contribute an uncertainty of 20% to both the absolute and relative values of the ozone densities. It is based upon magnetometer data and the assumption that at the end of thrust the rocket axis was aligned the velocity vector.

The largest source of error is in the character of the data, which contains noise from the photomultiplier dark current, stray pulses, and stars. It is difficult to separate this from the possible temporal and spatial variations of the airglow itself. A temporal variation could be responsible for some of the shape of the curve, but is is unlikely that the airglow would vary sufficiently in the 16 seconds of time that the ozone curve represents, to be responsible for its major features. Spatial variation is not thought to be a major source of uncertainty in the data since the numbers derived from the two photometers which were looking at different portions of the sky agree reasonably well. The magnitude of the noise-like errors

is apparent from the scatter of points about the curve and is on the order of 50%.

For comparison the daytime ozone distribution as measured by absorption of the solar spectra between 2500 and 3400 A [Johnson, et al, 1952] is shown. The daytime profile was computed using the ozone absorption coefficients of Ny and Choong [1933], which in the spectral region of interest are 10 to 15% higher than those of Inn and Tanaka used for the night time profile.

The most important feature of the profile is the factor of 6 increase in ozone density over the daytime profile above 60 km. While this may be in error by 50% or more, it is believed that the shape of the curve does indicate an increase of ozone density at night in this region, and that it is on the order of a half of a magnitude.

Techniques are being developed by various workers to use satellites for the measurement of ozone in this region. Venkateswaran [1961], observed the sunlight reflected from Echo I as it emerged from the earth's shadow, using various wavelength pairs between 4700 and 7000 A. His results above 55 km are about a factor of 15 higher than the measurements by Johnson, et al. However Venkateswaran [1963] states that this method probably gives too high values at levels above the principal ozone maximum.

The second type of observation was made at sunrise and sunset by a satellite borne radiometer with a response center at about 2630 A [Rawcliffe, et al, 1963]. At 60 km his data are about 20% lower than Johnson's, but approach Johnson's data, and above 80 km are somewhat higher than the trend of Johnson's data.

It is expected that the night time values would be higher. The magnitude of the effect, besides depending on reactions among the various oxygen species and third bodies, depends critically on such things as the initial hydrogen concentrations chosen [Bates and Nicolet, 1950, and Wallace, 1962] and possible reactions involving atomic nitrogen [Barth, 1961]. Perhaps the most recent computation of ozone densities has been done by B. G. Hunt [1964] using an atmosphere in which he assumes the only reactive constituent is oxygen. (The effects of atomic nitrogen and hydrogen would be to lower the calculated O and O_3 concentrations.) Between 40 and 50 km, Hunt's curve for just before sunrise conditions is as much as 30% lower than Johnson's daytime profile, crosses it at 53 km, and reaches a maximum value of 5×10^{10} molecules of O_3 per cm at 69 km.

AIRGLOW

The other principal result from the analysis of data from these photometers is information concerning the distribution of the airglow. Volume emission can be deduced

from the data obtained as the vehicle passes through the emitting region. The energy calibration of the photometers has been used in preparing these curves, (Figure 8) so that they do rightly represent the relative energy in the portion of the spectrum passed by the different filters. Ten arbitrary units represent on the order of one photon cm^{-2} sec^{-1} per A. The airglow as measured by the 2680 A photometer is 2.3 times that sensed by the 2620 A photometers. The airglow measured by the 2280 A photometers is 0.15 times that of the 2620 A photometers; nearly all the energy measured by the 2280 A photometers has come through a long wavelength tail of the filters. This pattern is completely consistent with a spectrum of the airglow horizon obtained by T. Ste[illegible]er with a spectrograph flown at 0030 local time on July [illegible], 1963.

The 2680 A filter was similar in construction and characteristics to those flown in March 1957 [Tousey, 1958] and November 1959 [Friedman, 1962, Packer, 1961]. The altitude of maximum emission were 101 and 96 km respectively, compared to 92 km for this flight. The zenith intensity for the 1957 flight was 3.4 rayleighs per Angstrom (Dunkelman, private communication) and for the 1959 flight was 1.04 rayleigh per Angstrom. The airglow during the flight of Aerobee 4.05 was somewhat brighter, but within a factor of 10 of these values.

The brighter stars and the Milky Way were readily noted in the records as the photometer scanned across the sky. The signal in the absence of obvious stars indicated that less than 15% of the light from extended sources originated above the emission layer indicated in Figure 8.

ACKNOWLEDGEMENTS

We thank the following colleagues at Goddard Space Flight Center for their help: Dr. A. Boggess III for making the data from his rocket payload available to us for this purpose; G. Baker and R.M. Windsor for the electronic instrumentation; E. Serra for engineering assistance in the payload preparation; T. Stecher for an advance copy of his airglow spectrum, without which the effective absorption cross section could not have been determined with significant accuracy; L. Dunkelman for the absolute values of the night airglow measurement in March 1957; and Dr. J.E. Kupperian, Jr. for his encouragement and suggestion of analysis of this data.

REFERENCES

Barth, C. A., Nitrogen and oxygen atomic reactions in the chemosphere, Chemical Reactions in the Lower and Upper Atmosphere, Stanford Research Institute, Interscience Publ., 303-326, 1961.

Bates, D. R., and M. Nicolet, The photochemistry of atmospheric water vapor, J. Geophys. Res., 55, 301-327, 1950.

Boggess III, A., Ultraviolet astronomical photometry from rockets, Space Astrophysics, W. Liller, ed., McGraw-Hill Book Co., 121-132, 1961.

Broida, H.P., and A. G. Gaydon, The Herzberg bands of O_2 in an oxygen afterglow and in the night-sky spectrum, Proc. Roy. Soc., London A222, 181-195, 1954.

Chamberlain, J.W., The ultraviolet airglow spectrum, Astrophys. J. 121, 277-286, 1955.

Chapman, S., On ozone and atomic oxygen in the upper atmosphere, Phil. Mag., 10, 369-383, 1930.

Chapman, S., A theory of upper-atmospheric ozone, Mem. R. Met. Soc., 3, 103-125, 1930.

Childs, C. B., Broad-band ultraviolet filters, J. Opt. Soc. Am., 51, 895-897, 1961.

DeMore, W. and O. Raper, Hartley band extinction coëfficients of ozone in the gas phase and in liquid nitrogen, carbon monoxide, and argon, J. Phys. Chem, 68, 412-414, Feb. 1964.

Dütsch, H. U., Current problems of the photochemical theory of atmospheric ozone, Chemical Reactions in the Lower and Upper Atmosphere, Stanford Research Institute, Interscience Publ., 167-180, 1961.

Friedman, H., A survey of NRL rocket research results obtained since the last COSPAR meeting, Space Research II, H.C. van de Hulst, ed., Interscience, N.Y. 1021-1035, 1961.

Hunt, B.G., A non-equilibrium investigation into the diurnal photochemical atomic oxygen and ozone variations in the mesosphere, W.R.E. Report, Tech. Note PAD 82, Feb. 1964 (Box 1424H, G.P.O. Adelaide, South Australia).

Inn, E.C.Y. and Y. Tanaka., Absorption coefficient of ozone in the ultraviolet and visible regions, J. Opt. Soc. Am., 43, 870-873, 1953.

Inn, E.C.Y., and Y. Tanaka, Ozone absorption coefficients in the visible and ultraviolet regions, Advan. Chem. Ser., No. 21, American Chemical Society, Washington, D.C., 263-268, 1959.

Johnson, F.S., J.D. Purcell, R. Tousey, and K. Watanabe, Direct measurements of the vertical distribution of atmospheric ozone to 70 kilometers altitude, J. Geophys. Res., 57, 157-176, 1952.

Nicolet, M., Nitrogen oxides and the airglow, The Threshold of Space, M. Zelikoff, ed., Pergamon Press, 40-57, 1957.

Ny, T.-Z., and S.-P. Choong,

Chinese J. Phys., 1, 38, 1933

Packer, D. M., Altitudes of the night airglow radiations, Ann. Geophys., 17, 67-75, 1961.

Paetzold, H.K., The photochemistry of the atmospheric ozone layer, Chemical Reactions in the Lower and Upper Atmosphere, Stanford Research Institute, Interscience Publ., 181-195, 1961.

Rawcliffe, R. D., G.E. Meloy, R.M. Friedman, and E.H. Rogers, Measurement of vertical distribution of ozone from a polar orbiting satellite, J. Geophys. Res. 68, 6425-6429, Dec. 15, 1963.

Tousey, R., Rocket Measurements of the Night Airglow, Ann. Geophys., 14, 186-195, April-June 1958.

Venkateswaran, S. V., J. G. Moore, and A. J. Krueger, Determination of the vertical distribution of ozone by satellite photometry, J. Geophys. Res., 66, 1751-1771, 1961.

Venkateswaran, S. V., On some problems of exploration of the upper atmosphere between 30 and 100 km by means of rockets and satellites, _Rocket and Satellite Meteorology: Proc. 1st Int'l. Symp. Rocket and Satellite Meteorology_, H. Wexler and J.E. Caskey, Jr., eds., John Wiley and Sons, 193-209, 1963.

Vigroux, E., Contribution a l'etude experimentale de l'absorption de l'ozone, _Ann. de Phys._, _8_, 709-762, 1953.

Wallace, L., The OH nightglow emission, _J. Atmos. Sci._, _19_, 1-16, 1962.

FIGURE CAPTIONS

Figure 1. Location of photometers on Aerobee 4.05.

Figure 2. Optical-electrical schematic of a photometer.

Figure 3. Spectral characteristics of flight filters.

Figure 4. Calibration curve for converter-amplifier.

Figure 5. Sample of telemetry record showing roll modulation of the airglow signal. Increasing signal represents increasing light.

Figure 6. Data from three photometers during the ascent of the rocket. The zenith angle is the angle between the longitudinal axis of the rocket and local zenith; the angle stated for each photometer is the angle between the photometer's optical axis and the rocket's longitudinal axis.

Figure 7. Altitude distribution of ozone.

Figure 8. Altitude distribution of the ultraviolet emission.

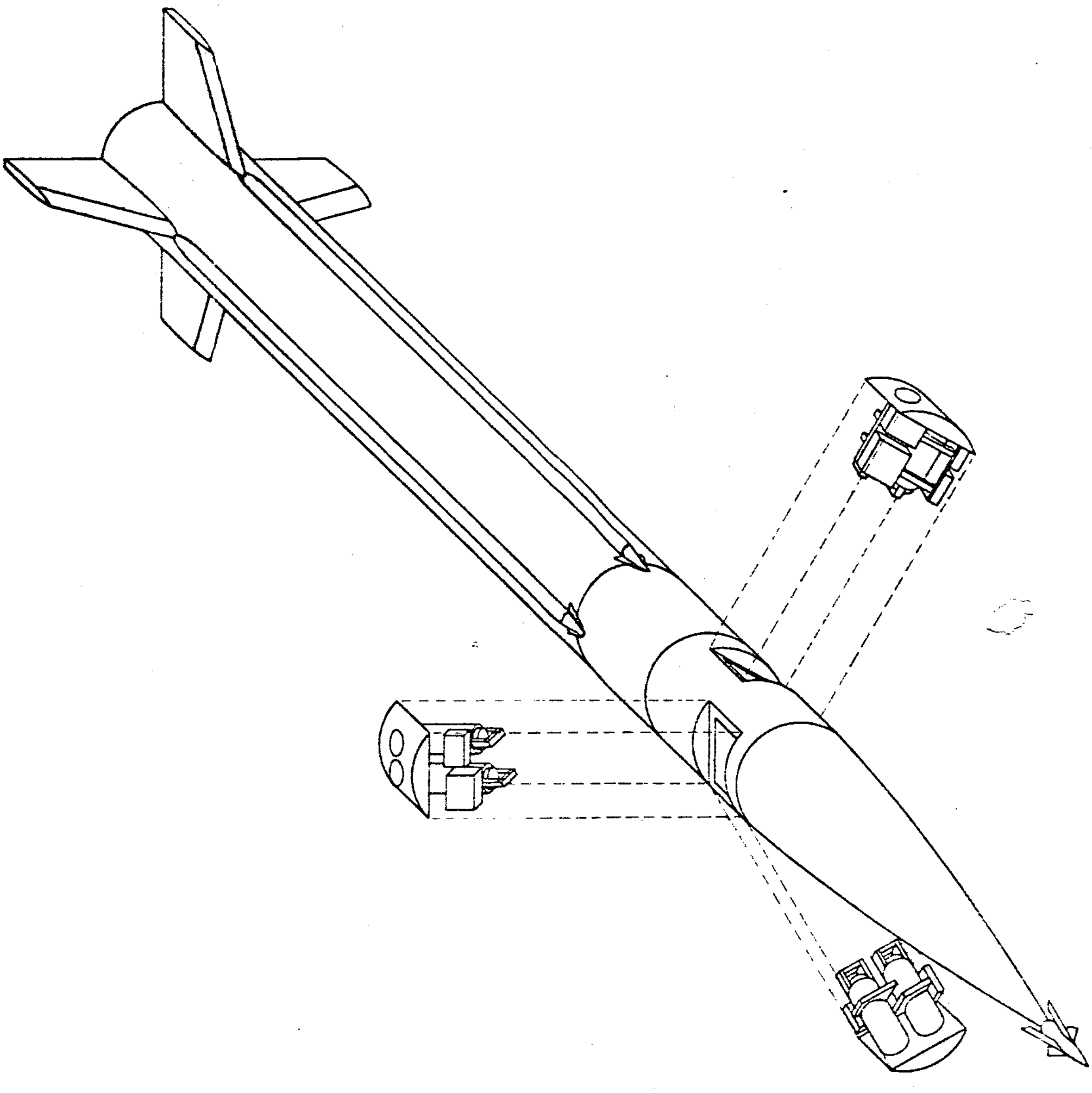

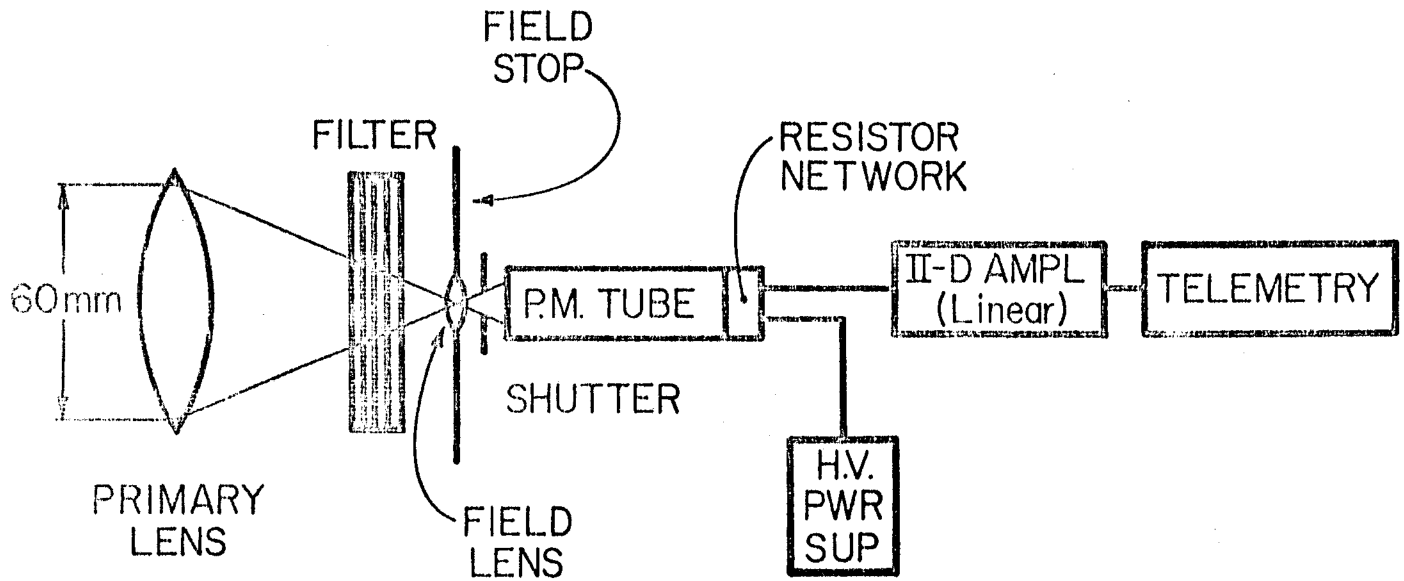
FIELD STOP
FILTER
RESISTOR NETWORK
60mm
P.M. TUBE
II-D AMPL (Linear)
TELEMETRY
SHUTTER
H.V. PWR SUP
PRIMARY LENS
FIELD LENS

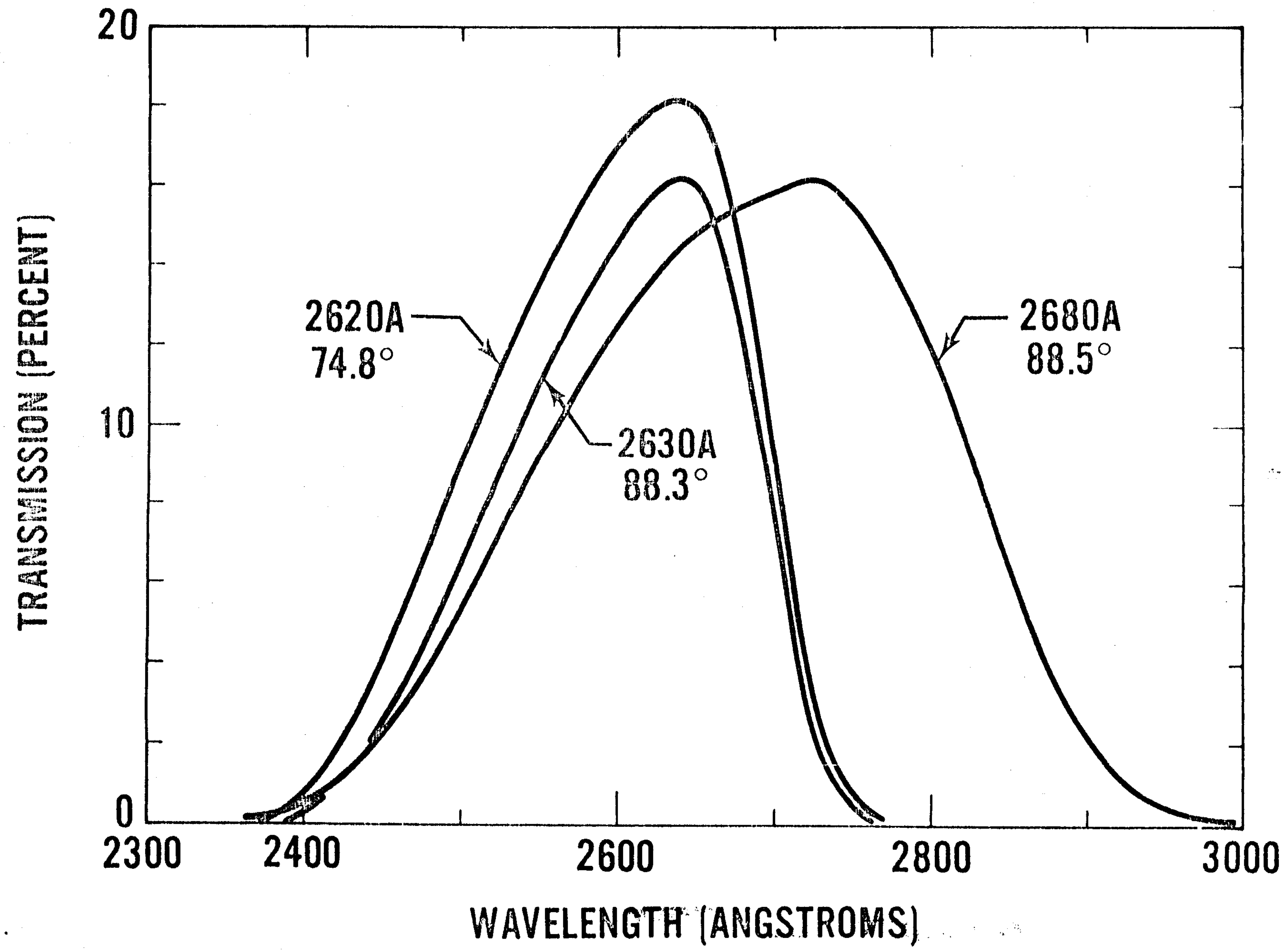
TRANSMISSION (PERCENT)
20
10
0
2300
2400
2600
2800
3000
WAVELENGTH (ANGSTROMS)
2620A
74.8°
2630A
88.3°
2680A
88.5°

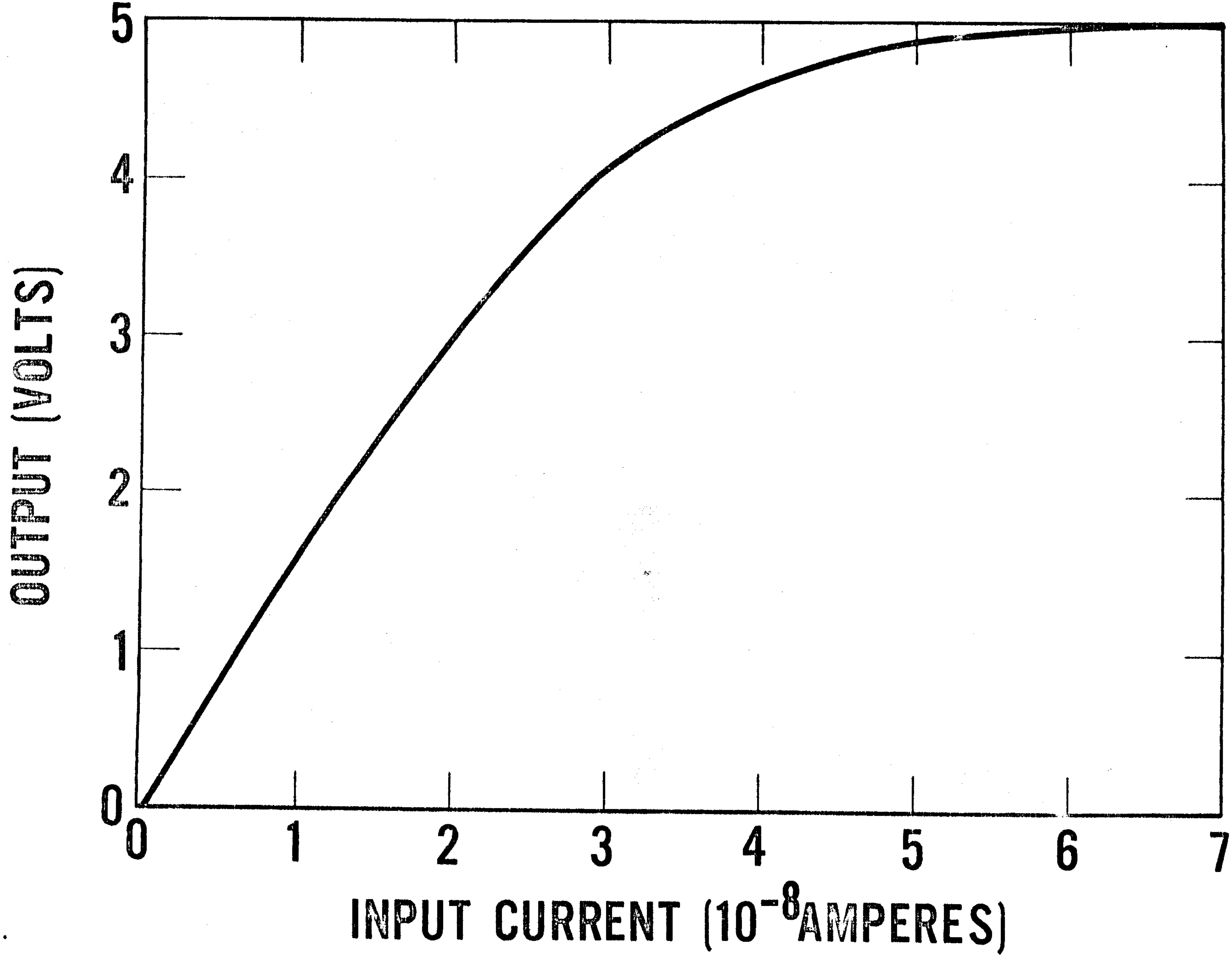

OUTPUT (VOLTS)
0
1
2
3
4
5
0
1
2
3
4
5
6
7
INPUT CURRENT (10^-8 AMPERES)

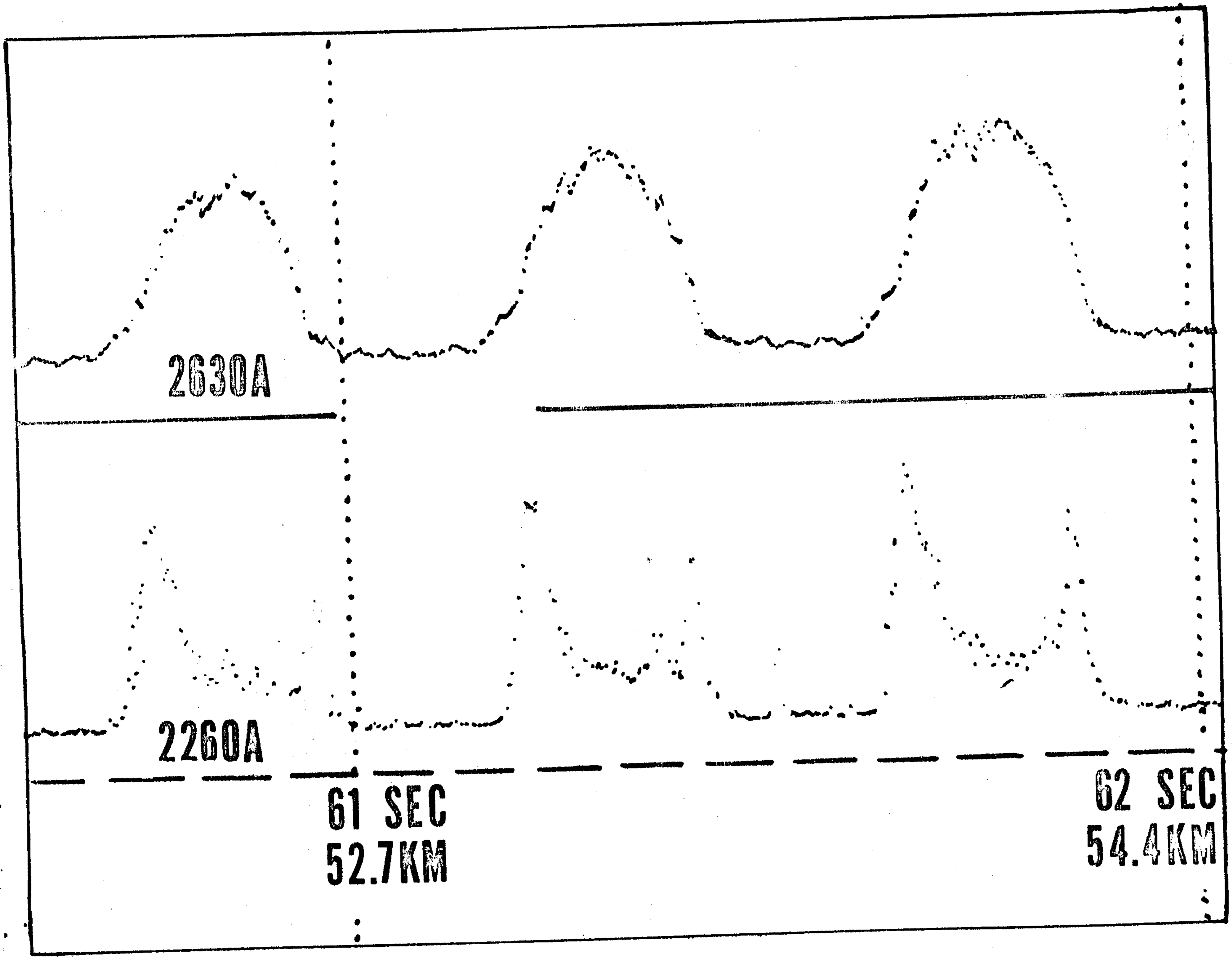
2630A
2260A
61 SEC
52.7KM
62 SEC
54.4KM

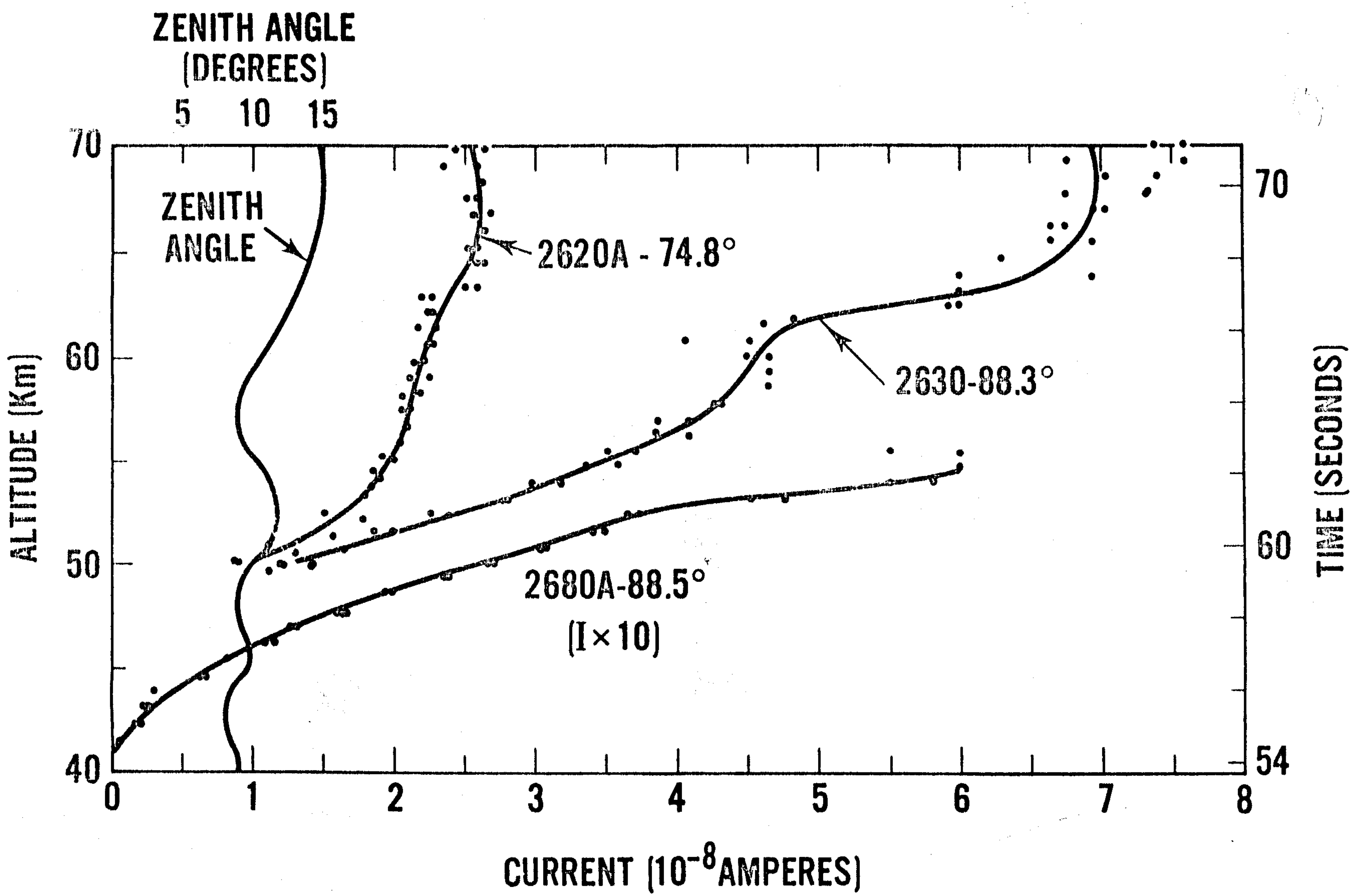

ZENITH ANGLE
(DEGREES)
5 10 15
ZENITH ANGLE
2620A - 74.8°
2630-88.3°
2680A-88.5°
(I×10)
ALTITUDE (Km)
40
50
60
70
TIME (SECONDS)
54
60
70
0 1 2 3 4 5 6 7 8
CURRENT (10^{-8}AMPERES)

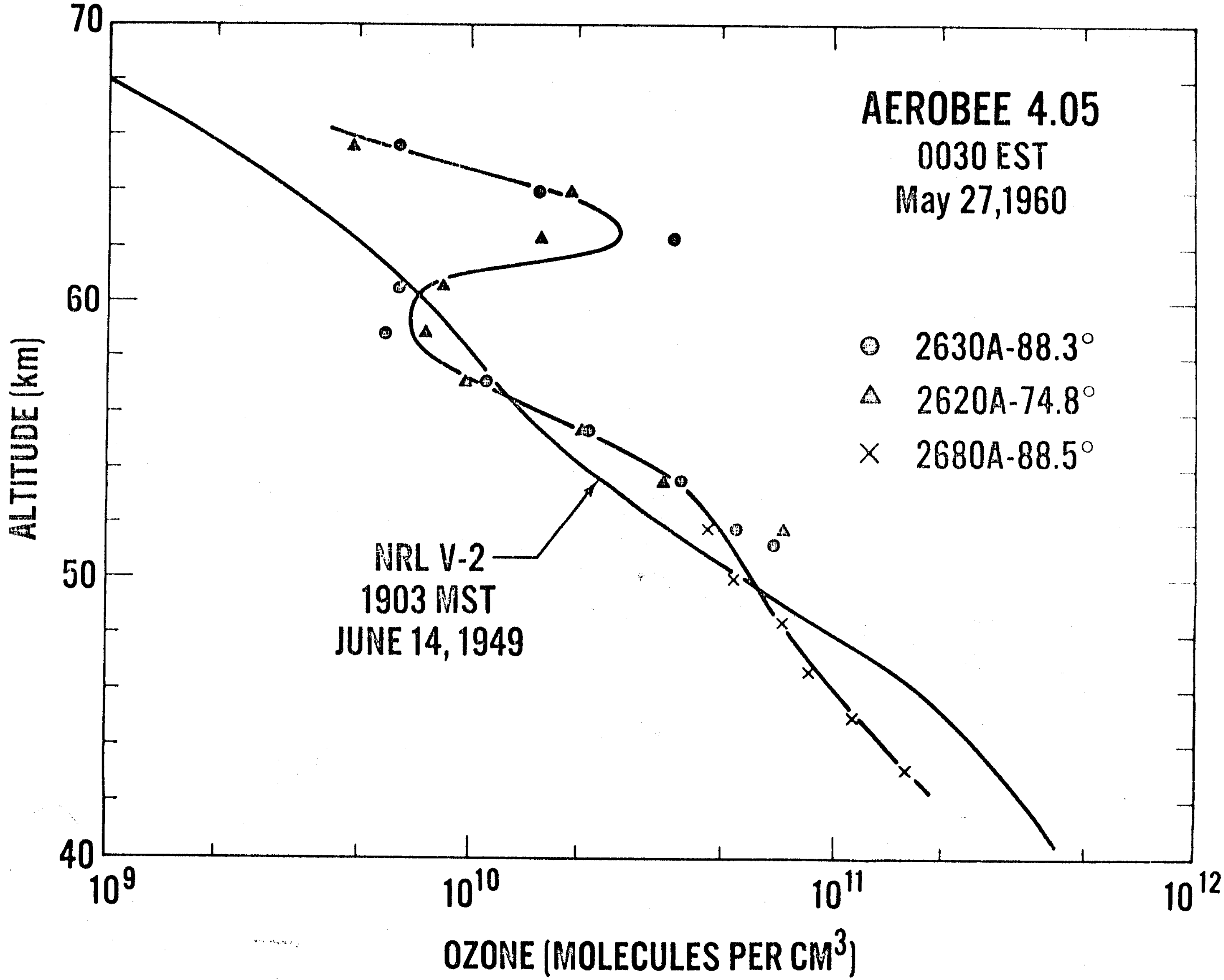
AEROBEE 4.05
0030 EST
May 27,1960
2630A-88.3°
2620A-74.8°
2680A-88.5°
NRL V-2
1903 MST
JUNE 14, 1949
70
60
50
40
ALTITUDE (km)
10^9
10^10
10^11
10^12
OZONE (MOLECULES PER CM^3)

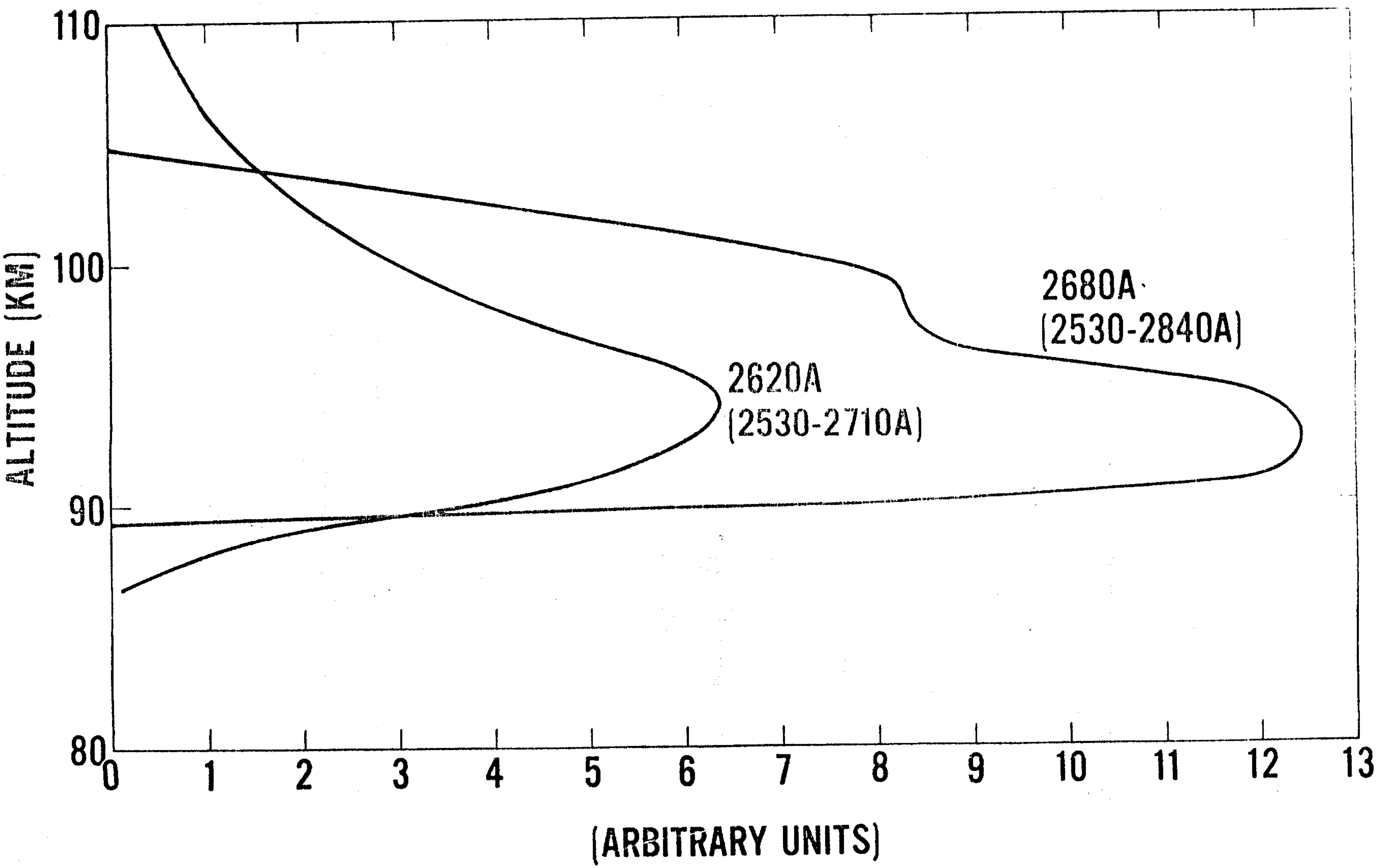
ALTITUDE (KM)
110
100
90
80
0
1
2
3
4
5
6
7
8
9
10
11
12
13
2620A
(2530-2710A)
2680A
(2530-2840A)
(ARBITRARY UNITS)